第 25 卷第 12 期　　半 导 体 学 报　　Vol. 25, No. 12
2004 年 12 月　　CHINESE JOURNAL OF SEMICONDUCTORS　　Dec., 2004

# Second-Order Raman Scattering from n- and p-Type 4H-SiC

Gao Xin[1], Sun Guosheng[1], Li Jinmin[1], Wang Lei[1], Zhao Wanshun[1], Zhang Yongxin[2] and Zeng Yiping[1]

(1 *Novel Semiconductor Material Laboratory, Institute of Semiconductors, The Chinese Academy of Sciences, Beijing 100083, China*)
(2 *School of Physical Science and Technology, Lanzhou University, Lanzhou 730000, China*)

**Abstract**: The results of second-order Raman-scattering experiments on n- and p-type 4H-SiC are presented, covering the acoustic and the optical overtone spectral regions. Some of the observed structures in the spectra are assigned to particular phonon branches and the points in the Brillouin zone from which the scattering originates. There exists a doublet at 626/636cm$^{-1}$ with energy difference about 10cm$^{-1}$ in both n- and p-type 4H-SiC, which is similar to the doublet structure with the same energy difference founded in hexagonal GaN, ZnO, and AlN. The cutoff frequency at 1926cm$^{-1}$ of the second-order Raman is not the overtone of the $A_1$(LO) peak of the n-type doping 4H-SiC, but that of the undoping one. The second-order Raman spectrum of 4H-SiC can hardly be affected by doping species or doping density.

**Key words**: 4H-SiC; second-order Raman; cutoff frequency
**PACC**: 7280J; 3220F
**CLC number**: O472.3　　**Document code**: A　　**Article ID**: 0253-4177(2004)12-1555-06

## 1 Introduction

In recent years silicon carbide has become a subject of intensive experimental and theoretical studies. The interest in this semiconductor is due to its wide energy gap, high thermal conductivity, and large breakdown electric field, which make it a promising material for high-temperature electronic devices. Various polytypes of SiC have different application fields, but the hexagonal 4H-SiC crystals with their relatively high electron mobility and almost isotropic electric conduction seem to be the best for electronic applications[1].

In contrast to the first-order Raman measurements which are sensitive only to phonons at the Γ point ($k$= 0) of Brillouin zone (BZ), second-order experiments provide information on the vibrational states throughout the entire Brillouin zone, which is important in considering, for example, the electronic conduction or the nonradiative relaxation processes of electrons. Second-order Raman spectra are a sensitive test of theoretical models of the lattice dynamics, because typically they are continuous spectra with peaks corresponding to regions or points of dispersion curve with zero gradient and hence maxima in the phonon density of states[2~4].

Burton *et al.*[5] studied the second-order Raman spectra of n-type 4H-SiC, but there are no reports on p-type one until now. In this study, we presented the second-order Raman spectra of p-type and n-type doped 4H-SiC. The spectral region investigated contains the acoustic as well as the optical overtone and combination band.

Gao Xin　male, was born in 1972, PhD candidate. His works focus on SiC semiconductor material engineering and devices. Email: gaoxin@red.semi.ac.cn

Received 24 March 2004, revised manuscript received 8 July 2004

## 2 Experiment

The samples investigated were about 2.5~3μm-thick epilayers grown homoepitaxially on 8° off-axis n-type 4H-SiC(0001) substrates (10mm×10mm) from Cree inc by chemical vapor deposition (CVD). A specular surface of the epilayers was observed by Nomarski microscopy, and AFM showed a very low roughness ranging from 0.3 to 0.36nm in the area of 5μm×5μm. The two n-type epilayers were nitrogen doped with nominal doping concentrations of $4.7\times10^{17}$ (sample N1) and $6.5\times10^{18}$ $cm^{-3}$ (sample N2), respectively, and the p-type epilayer aluminum doped with nominal doping concentration of $2.4\times10^{18}cm^{-3}$ (sample P). The Raman-scattering experiments were carried out at room temperature using the 488nm line of an Ar ion laser for excitation, and a charge-coupled-detector (CCD) was used to detect weak signals. The laser beam was focused onto the sample surface by means of a high magnification microscope objective, which was also used to collect the scattered light. Collection geometry was in the near backscattered configuration perpendicular to the (0001) face of the sample. Small deviations from the true backscattering geometry could be expected due to the high numerical aperture (NA) of the objective, which was a ×100, with NA = 0.95. The excitation spot onto the sample surface was in the order of a micrometer in size. The polarization was unspecified both for incident and collected light.

## 3 Results and discussion

Similar to all known SiC polytypes, 4H-SiC is an indirect band-gap semiconductor and belongs to the point group $C_{6v}^4$ having eight atoms per unit cell. Group-theoretical analysis shows that the Raman-active modes of a wurtzite structure, which has $C_{6v}$ symmetry, are the $A_1$, $E_1$, and $E_2$ modes[6]. The $A_1$ and $E_1$ phonon modes, which are also infrared(IR) active, are spit into longitudinal optical (LO) and transverse optical (TO) modes. In a backscattering geometry, where the incident and collected light are parallel to the *c* axis of the sample, the $A_1$(LO), $E_1$(TO), and $E_2$ phonons are expected to be seen in the Raman spectra at excitation energies which are nonresonant[6,7]. Figure 1 shows typical Raman data for p-type 4H-SiC, taken at room temperature. The major peaks in the 4H-SiC Raman spectra are identifiable from previous studies[8]. The high quality of the data obtained in our experiments allows the observation of several weaker peaks present in the Raman spectra. These additional peaks, with symmetry identification, are also listed in Table 1.

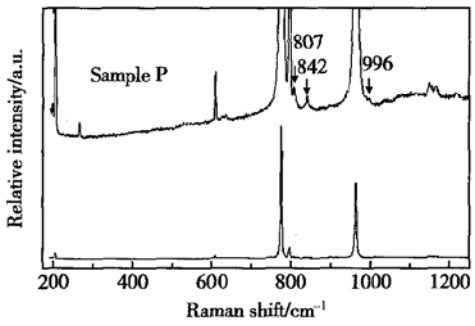


Fig. 1 Raman spectra of p-type 4H-SiC recorded at room temperature in backscattering geometry The upper curve is a spectrum with an enlarged *y* scale to show details.

Table 1 Peak assignments for the first-order Raman spectrum shown in Fig. 1

| 4H-SiC peak Raman shift/$cm^{-1}$ | Mode symmetry | Reduced wave vector $x=q/q_B$ |
|---|---|---|
| 195.5 | $E_2$ planar acoustic | 2/4 |
| 203.5 | $E_2$ planar acoustic | 2/4 |
| 266.0 | $E_1$ planar acoustic | 4/4 |
| 610.5 | $A_1$ axial acoustic | 4/4 |
| 777.0 | $E_2$ planar optic | 2/4 |
| 797.5 | $E_1$ planar optic | 0 |
| 838.0 | $A_1$ axial optic | 4/4 |
| 964.5 | $A_1$ axial optic | 0 |

The total spectra can be divided into two parts: the low-frequency region of the spectra (approximately 500~1250$cm^{-1}$) is dominated by acoustic overtones; and the second-order optical

bands lie in the high-frequency portion of the spectra (approximately 1455~ 2000cm$^{-1}$). The corresponding spectra are shown in Figs. 2 and 3, respectively.

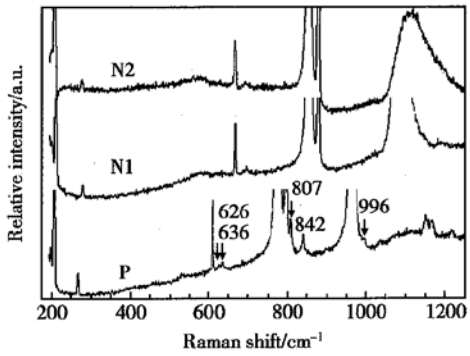


Fig. 2　Second-order room-temperature Raman spectra of n- and p-type 4H-SiC in the low-frequency region　The polarization is unspecified both for incident and collected light.

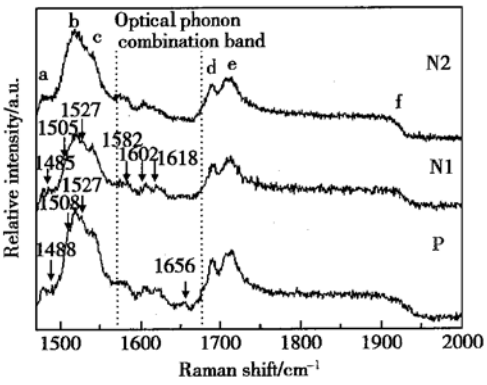


Fig. 3　Second-order room-temperature Raman spectra of n- and p-type 4H-SiC in the high-frequency region, under the same conditions as shown in Figs. 1 and 2

In the following we discuss the strongest experimentally observed structures for each region.

### 3.1　Low-frequency region: acoustic overtones

The low-frequency region is shown in Fig. 2. One can note a feature in the Raman spectra in the n- and p-type samples, which starts at around 500 cm$^{-1}$ and extends past 1000 cm$^{-1}$. Burton *et al.* [5] assigned these features as the acoustic branch of the two-phonon Raman spectrum. It can be seen that the spectrum of the p-type 4H-SiC exhibits richer structure of phonon modes than that of the n-type one. Three distinct peaks appear only in p-type 4H-SiC at 807, 842, and 996cm$^{-1}$. The other peaks at about 530cm$^{-1}$, doublet 626/636cm$^{-1}$ and around 1060~ 1250cm$^{-1}$ are common in both p- and n-type samples. The peak at around 1100~ 1250cm$^{-1}$ in the sample N2 cannot be observed clearly, probably obscured by first-order LO phonon plasmon coupled (LOPC) modes in SiC.

A broad peak appears at around 530cm$^{-1}$. From its line shape and its low frequency one can assign the 530cm$^{-1}$ mode to an overtone process of acoustic phonons. As can be seen in the theoretically calculated phonon dispersion curves in Ref. [9], the energy position as well as the observed symmetry fits well with the flat phonon branch at the *M* point in the Brillouin zone. This is emphasized by the fact that this mode was not observed in cubic SiC[3,10]. It is noteworthy that a doublet with a small energy difference of 10cm$^{-1}$ also exists in hexagonal GaN[11], ZnO[12], and AlN[13]. According to the calculated phonon-dispersion curves in Ref. [9] the doublet in question can be attributed to an overtone of transverse acoustic phonons at the high symmetry point *M* in the Brillouin zone, corresponding to around 313cm$^{-1}$ mode and 318cm$^{-1}$ mode, respectively. The energies of the two modes agree excellently with the acoustic phonon energies of 41.1 and 41.9meV at the *M* point obtained by the low temperature photoluminescence (LTPL)[14]. Other peaks at around 1100 ~ 1250cm$^{-1}$ can be attributed to an overtone process of the highest acoustic-phonon branches at the zone boundary *M* point and at the zone center Γ point. These peaks do not exhibit any change as nitrogen concentration is varied, thus none of them are due to local mode vibrations of the nitrogen. However there some new peaks exist in p-type sample. It could not be confirmed presently whether these peaks in p-type sample are related to local modes of the aluminum atoms, or to the defect-induced Raman scattering signals[15,16]. In the LTPL of the sample P, however, the defect-related

PL lines were clearly observed. So the authors tend to conjecture that these peaks are brought about by the stacking faults existing in the sample P, which cause breakdown of the wave-vector selection rule, thus providing appearance of new Raman bands.

### 3.2 High-frequency region: optical combinations and overtones

The optical combination and overtone region is shown in Fig. 3. The frequencies of the observed second-order Raman features together with their assignments are listed in Table 2. The spectra structures were similar in both of n- and p-type samples, and also similar to that of semi-insulating 4H-SiC[5]. Some small discrepancies exist, however, and may be due to the way the spectra were recorded or due to differences in material quality.

Table 2 Frequencies (in units of $cm^{-1}$) and symmetries of the strongest modes found in the second-order Raman spectra of 4H-SiC and their assignments

| SI* | N1 | N2 | P | Label | Symmetry |
|---|---|---|---|---|---|
| 1475 | 1478 | 1478 | 1478 | a | *K* |
| | 1485 | | 1488 | | *K* |
| | 1505 | | 1508 | | *K* |
| 1515 | 1516 | 1517 | 1518 | b | *L* |
| | 1527 | 1527 | 1527 | | *L*-*M* |
| | | | | | Branch |
| 1542 | 1540 | 1541 | 1543 | c | *M* |
| 1577 | 1578 | 1577 | 1578 | | |
| 1606 | 1604 | 1603 | 1604 | | Phonon |
| 1622 | 1620 | 1617 | 1618 | | Combination |
| | | | 1625 | | Bands |
| 1654 | 1653 | 1654 | 1654 | | |
| 1689 | 1691 | 1689 | 1690 | d | *M* |
| 1714 | 1713 | 1714 | 1714 | e | *M*, *L* |
| 1925/1930 | | | | | |
| | 1926 | 1926 | 1926 | f | $\Gamma = A_1(LO)$ |

* SI denotes semi-insulating 4H-SiC from Ref. [5]

The structures located at $1478cm^{-1}$ (labeled a), $1485cm^{-1}$ and $1505cm^{-1}$ are probably a consequence of the flatness of the dispersion curve of 4H-SiC at the point *K* of BZ. Considering the energy position of the peak $1478cm^{-1}$, it should be the overtone of $739cm^{-1}$ at the point *K*. Theoretical calculation of the phonon dispersion curve has shown that the lowest point in the optical branch is the *K* point phonon[9]. So the optical branch of the overtone spectrum should begin at $1478cm^{-1}$ for 4H-SiC.

As is the case in other hexagonal or cubic semiconductors the highest-frequency second-order Raman signal originates from optical-phonon overtones[17~19]. The highest-energy distribution of the second-order Raman signal with a cutoff at $1926cm^{-1}$ (labeled f) is attributed to an overtone of the zone-center $A_1(LO)$ mode at $\Gamma$ point. It can be noted that the overtones of the $A_1(LO)$ in both n- and p-type 4H-SiC have the same cutoff at $1926cm^{-1}$, though the peak positions of $A_1(LO)$ have noticeable difference for the three samples, N1 at $972cm^{-1}$, N2 at $1009cm^{-1}$, and P at $964cm^{-1}$, respectively. So the cutoff frequency of second-order Raman scattering in 4H-SiC is not equal to the overtones of the $A_1(LO)$ peaks of n-type doping 4H-SiC samples obtained experimentally, but only determined by that of the $A_1(LO)$ peak from undoping 4H-SiC. Based on the above observations, it can be concluded that unlike $A_1(LO)$ modes in the first-order Raman spectrum the cut-off frequency of the second-order Raman signal for 4H-SiC can hardly be affected by doping species or doping density.

Burton *et al.*[5] had assigned the $1515cm^{-1}$ (labeled b) as the overtone of the *L* point phonon at 758 and $1542cm^{-1}$ (labeled c), 1688 (labeled d) and $1714cm^{-1}$ (labeled e) as the overtones of the *M* symmetry phonons at 771, 840, and $857cm^{-1}$, respectively. According to the theoretically calculated phonon frequencies on high symmetry points *L* and *M* for 4H-SiC[20], however, the broad peak at around $1714cm^{-1}$ may also arise from an overtone of the *L* point phonon at $856cm^{-1}$, 2LO (*L*) ($1712cm^{-1}$), which can be substantiated by the flat phonon branch at the *L* point in the BZ[9].

In Ref. [5] the peak at around $1526cm^{-1}$ can be clearly observed only in the 6H-SiC spectrum, but in the present Raman spectra for the 4H-SiC the peak at $1527cm^{-1}$ appeared obviously. The peak

locating between 2LO($L$) and 2LO($M$) cannot be fitted with an overtone combination of optical phonons at $L$ or $M$ point. The modes at the $L$ point are twofold degenerate and the degeneracy is lifted along the $L$-$M$ branch. The maximum splitting is generally reached at the $M$ point whereas there exist intermediate values falling between 2LO($L$) and 2LO($M$). It suggests that the peak at 1527cm$^{-1}$ arises from an overtone of an optical phonon with wave vector on the $L$-$M$ branch. The dispersion curves of the optical phonons for wave vectors between the points $L$ and $M$[9] are very flat, and consequently the density of states for two phonon processes is expected to be large.

A region between 1580cm$^{-1}$ and 1680cm$^{-1}$ exhibits a rich structure of less intensive modes. The strongest features are the structures around 1582, 1602, 1618, and 1656cm$^{-1}$. The 1656cm$^{-1}$ mode is only detected in the sample P and the 1618cm$^{-1}$ mode cannot be clearly identified in the heavily doping sample N2. All these modes can be attributed to second-order Raman-scattering processes. The theoretical calculation shows that there exists a gap in phonon density of states approximately between 785cm$^{-1}$ and 840cm$^{-1}$[9]. It extends in the overtone spectrum from 1570cm$^{-1}$ to 1680cm$^{-1}$. Thus these peaks appearing in the region for 4H-SiC must be due to combinations of phonons from different branches and cannot be caused by optical overtones.

## 4 Summary

The second-order Raman-scattering results of n- and p-type 4H-SiC were presented. The seconds order Raman spectrum structures of both n- and p-type samples were found to be quite similar. The author assigned some of the observed structures in the spectra to particular phonon branches and determined the points in the Brillouin zone from which the scattering originates. There exists a doublet with a small energy difference about 10cm$^{-1}$ in 4H-SiC, which is similar to that of hexagonal GaN, ZnO and AlN. We find the cutoff frequency is not determined by the overtone of the $A_1$(LO) of the n-type doping 4H-SiC, but by that of the undoping one. The p-type aluminum doping 4H-SiC shows the similar second-order Raman spectrum structures to that of n-type nitrogen doping one, and the nitrogen doping density has less effect on the second-order spectra.

## References


[1] Schaffer W J, Negley G H, Irvine K G, et al. Conductivity anisotropy in epitaxial 6H and 4H-SiC. Mater Res Soc Symp Proc, 1994, 339: 595

[2] Yu P Y, Cardona M. Fundamentals of semiconductors. New York: Springer-Verlag, 1996

[3] Windl W, Karch K, Pavone P, et al. Second-order Raman spectra of SiC: experimental and theoretical results from ab initio phonon calculations. Phys Rev B, 1994, 49: 8764

[4] Karch K, Bechstedt F, Pavone P, et al. Pressure-dependent properties of SiC polytypes. Phys Rev B, 1996, 53: 13400

[5] Burton J C, Sun L, Long F H. First- and second-order Raman scattering from semi-insulating 4H-SiC. Phys Rev B, 1999, 59: 7282

[6] Hayes W, Loudon R. Scattering of light by crystals. New York: Wiley, 1978

[7] Cardona M, Guntherodt G. Light scattering in solids Ⅱ. New York: Springer, 1982

[8] Feldman D W, Parker J H, Choyke W J, et al. Raman scattering in 6H-SiC. Phys Rev, 1968, 170: 698

[9] Hofmann M, Zywietz A, Karch K, et al. Lattice dynamics of SiC polytypes within the bond-charge model. Phys Rev B, 1994, 50: 13401

[10] Olego D, Cardona M. Pressure dependence of Raman phonons of Ge and 3C-SiC. Phys Rev B, 1982, 25: 1151

[11] Siegle H, Kaczmarczyk G, Filippidis L, et al. Zone-boundary phonons in hexagonal and cubic GaN. Phys Rev B, 1997, 55: 7000

[12] Hewat A W. Lattice dynamics of ZnO and BeO. Solid State Commun, 1970, 8: 187

[13] Karch K, Portisch G, Bechstedt F, et al. Ab initio calculation of structural and dynamical properties of AlN. Inst Phys Conf Ser, 1996, 142: 967

[14] Ivanov I G, Lindefelt U, Henry A, et al. Phonon replicas at the $M$ point in 4H-SiC: A theoretical and experimental study. Phys Rev B, 1998, 58: 13634

[15] Nakashima S, Nakatake Y. Detection of stacking faults in 6H-SiC by Raman scattering. Appl Phys Lett, 2000, 77: 3612

[16] Nakashima S, Y Nakatake Y, Ishida Y, et al. Sensitive detec-

tion of defects in α and β SiC by Raman scattering. Materials Science Forum, 2002, 389~ 393: 629

[17] Gorban I S, Lugovoi V I. Second-order Raman spectra in silicon carbide crystals. Spektrosk, 1976, 24: 333

[18] Temple P A, Hathaway C E. Multiphonon Raman spectrum of silicon. Phys Rev B, 1973, 7: 3685

[19] Weinstein B A, Cardona M. Second-order Raman spectrum of germanium. Phys Rev B, 1973, 7: 2545

[20] Bechstedt F, Käckell P, Zyweitz A, et al. Polytypism and properties of silicon carbide. Phys Status Solidi B, 1997, 202: 35

# n 型和 p 型 4H-SiC 的二级喇曼谱

高 欣[1] 孙国胜[1] 李晋闽[1] 王 雷[1] 赵万顺[1] 张永新[2] 曾一平[1]

(1 中国科学院半导体研究所 新材料实验室, 北京 100083)

(2 兰州大学物理学院, 兰州 730000)

**摘要**: 给出了 n 型和 p 型 4H-SiC 的二级喇曼谱的实验结果. 指认了所观察到的一些光谱结构对应的特定声子支及其在布里渊区中相应的对称点. 发现在 4H-SiC 的二级喇曼谱中存在能量差约为 10cm$^{-1}$的双谱线结构, 这一结构与六方相 GaN, ZnO 和 AlN 的双谱线结构具有相同的能量差. 二级喇曼谱的截止频率对于不同掺杂情况的 4H-SiC 具有相同的值. 它并不等于 n 型掺杂 4H-SiC 的 $A_1(LO)$ 声子的倍频, 而是等于未掺杂样品的 $A_1(LO)$ 声子的倍频. 掺杂类型和杂质浓度对 4H-SiC 的二级喇曼谱几乎没有影响.

**关键词**: 4H-SiC; 二级喇曼谱; 截止频率

**PACC**: 7280J; 3220F

**中图分类号**: O472.3 **文献标识码**: A **文章编号**: 0253-4177(2004)12-1555-06

高 欣 男, 1972 年出生, 博士研究生, 主要从事 SiC 半导体材料生长和器件研究.

2004-03-24 收到, 2004-07-08 定稿